JOINT INSTITUTE FOR NUCLEAR RESEARCH

Dzhelepov laboratory of Nuclear Problems

FINAL REPORT ON THE INTEREST PROGRAMME

Energy and spatial resolutions of a large volume LS detector

Supervisor:
Dr. Oleg Yurievich Smirnov

Student:
Kirill Kiselev, Russia
National Research Nuclear University "MEPHI"

Participation period:
November 5 – December 14,
Wave 11

Dubna, 2024

ABSTRACT

Modern large scintillation detectors are designed and used to study a plethora of physical problems in the course of the experiment. To accurately conduct the research with these detectors, they need to have good energy and spatial resolutions. Continuing the work started in the START Programme, we create a «fast event generator» for the JUNO detector, which uses an analytical approximation of the PMT light collection function to bypass the process of tracking each scintillation photon individually. Additionally, we develop a method of reconstructing the coordinates of individual events, using the positions and the signal arrival times of the PMTs in the event.

CONTENTS

INTRODUCTION

THE JUNO DETECTOR

JUNO (Jiangmen Underground Neutrino Observatory) is a large underground liquid scintillator detector located in an underground laboratory under the Dashi hill (700 m underground) in Jinji town in Guangdong province, China [1]. The primary physics goal of the JUNO detector was proposed to be the determination of the neutrino mass ordering [2], however other neutrino oscillation and astroparticle physics topics will be researched.

The Central Detector (CD) of JUNO will be a spherical acrylic vessel 35.4 m in inner diameter and 120 mm thick containing 20 kton LAB-based (linear alkylbenzene) liquid scintillator and supported by a spherical stainless steel (SS) structure (see fig. 1). The CD volume will be watched by 17612 20-inch "large" PMTs (photomultiplier tubes) and 25600 3-inch "small" PMTs. The cylindrical Water Pool (WP), in which the CD will be contained, will be filled with 35 ktons of ultrapure water and will be watched by 2400 20-inch PMTs to create a Cherenkov detector for vetoing muons. Also a part of the veto, the Top Tracker (TT) will be located above the main detector and will consist of plastic scintillating strips.

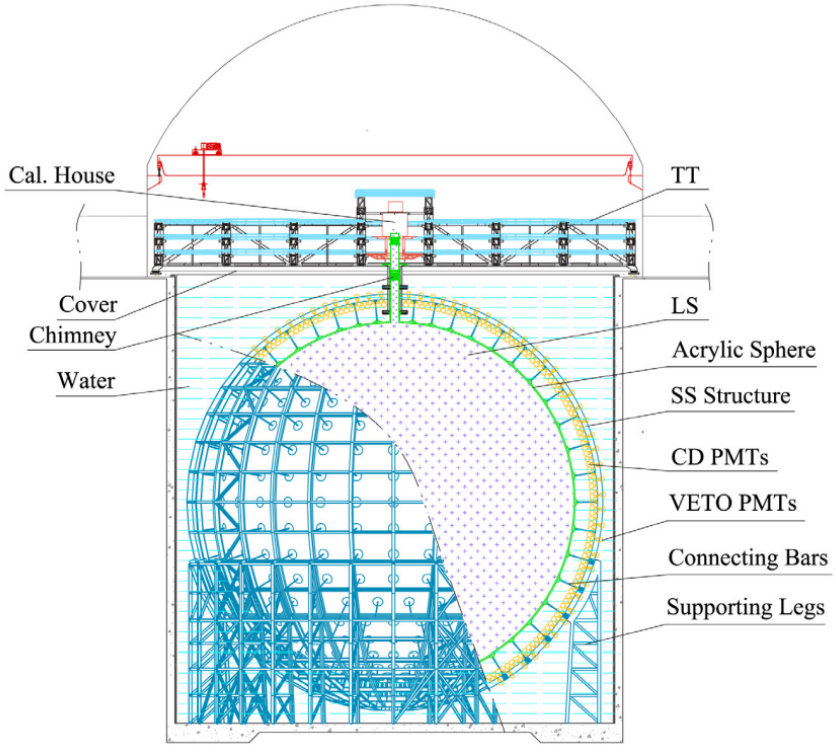

Fig. 1 — Schematic view of the JUNO detector [1]

DETECTOR RESPONSE MODELING

Usually the response of a detector is modelled using toolkits such as Geant4, which allow to simulate the geometry of the detector, its materials and the passage of particles through it. Such methods are used ubiquitously: in high energy, nuclear and neutrino physics, medical science, etc. It allows for detailed event generation, e.g. in a given scintillation event the path of each photon through matter is tracked from its emission to its capture in the detector and then the response of detector electronics is also simulated. This way of modeling, while being very thorough and giving large amounts of data for preliminary and ongoing study of the detector, can be quite slow, taking seconds to generate a single event, while in a real detector event frequency may easily measure in thousands per second.

A more «phenomenological» path of event generation was used in the CTF experiment [3; 4] and discussed in [5]: it consists of defining an analytical approximation of the detector response with some free parameters, evaluating their values from fitting the approximation to real or generated data and then quickly generating events based on the approximation. Here a similar analysis is reported for the generated data of the JUNO detector.

1 FAST EVENT GENERATOR

A preliminary analysis was conducted during the course of the START programme [6]. The results of that work are used in this study. A brief explanation of the study and its results is presented in section 1.1 of this report.

1.1 LIGHT COLLECTION MAP

1.1.1 JUNO CD PHOTOMULTIPLIER TUBES

In JUNO detector and in the software used for the analysis the 17612 large 20-inch photomultiplier tubes (LPMTs) are divided into three types: NNVT (2720 PMTs), HighQENNVT (9825 PMTs) and Hamamatsu (4997 PMTs). The first two types are both Microchannel Plate Photomultipliers and thus have similar physical properties, the latter type are dynode PMTs. All LPMTs are fixed on spherical a metal frame at the distance of $L_0 = 19.4$ m from the center the CD of JUNO detector (fig. 1.1).

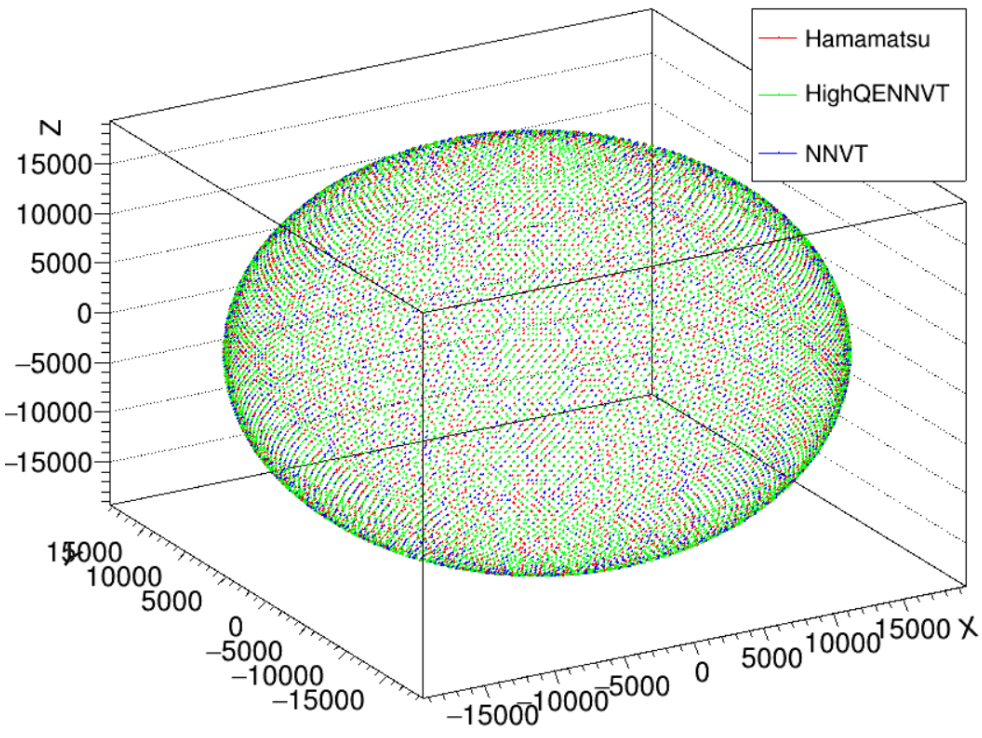

Fig. 1.1 — The arrangement of PMTs in JUNO CD by type: Hamamatsu (red), HighQEN-NVT (green) and NNVT (blue). The coordinates are measured in mm.

The coordinates of a given PMT point to the geometric center of the photocathode surface. In this analysis however, we will use the coordinates of the «top» of the PMT photocathode surface — the closest point to the center of the detector. These can be calculated if the distance between the two points for each LPMT type is known: ∼190 mm for Hamamatsu and ∼184 mm for NNVT.

1.1.2 THE AVERAGE CHARGE FOR AN EVENT IN THE CENTER OF CD

As will be seen later, the PMT light collection map is normalized to the center of the CD volume as the JUNO detector volume is spherically symmetrical. To estimate the charge collected by each LPMT in a point-like event at the center of the detector, we first generated $N_{ev} = 10^5$ events of 1 MeV single electrons, calculated the average charge collected by the whole detector per event $\langle Q_0 \rangle$ (in photoelectrons — p.e.) and then divided it by the total number of LPMTs:

$$\mu_0 = \frac{\langle Q_0 \rangle}{N_{PMT}}. \tag{1.1}$$

The error of μ_0 value can be calculated accounting for the variance of signal multiplication in PMTs due to its statistical nature. Each photoelectron, multiplied by the PMT dynode system, creates a slightly different signal in the outer circuit. This results in an increase in the variance of the output signals relative to the input signals. The factor by which the variance increases is called the excess noise factor (ENF), which has been measured for the PMTs of the JUNO detector [7]. The measured ENF is 1.19 for Hamamatsu PMTs and 1.58 for NNVT PMTs. Then the error:

$$\Delta\mu_0 = \Delta\left(\frac{\langle Q_0 \rangle}{N_{PMT}}\right) = \frac{\Delta\langle Q_0 \rangle}{N_{PMT}} = \frac{1}{N_{PMT}}\sqrt{\frac{\mathrm{ENF}\cdot\langle Q_0 \rangle}{N_{ev}}} \tag{1.2}$$

Another way to calculate μ_0 is to extract it from the number N of LPMTs that registered at least 1 p.e.. The distribution of the number of p.e., registered by a single LPMT follows the Poisson law with the average value of μ_0. Then we can calculate:

$$\mu_0 = -\ln\left(1 - \frac{N}{N_{trig}}\right), \tag{1.3}$$

$$\Delta\mu_0 = \Delta\left(-\ln\left(1 - \frac{N}{N_{trig}}\right)\right) = \frac{N_{trig}}{N_{trig} - N}\frac{\Delta N}{N_{trig}} = \sqrt{\frac{N}{N_{trig}(N_{trig} - N)}}, \tag{1.4}$$

where $N_{trig} = N_{ev} \cdot N_{PMT}$ — the total number of triggers (the number of times a PMT could have registered a signal)

As there are 17612 LPMTs watching the CD and the expected yield of photons in

JUNO per scintillation event is $\sim 1600\frac{\text{p.e.}}{\text{MeV}}$ [1], the value of μ_0 is $\approx 0.1\frac{\text{p.e.}}{\text{MeV}\cdot\text{event}\cdot\text{PMT}}$. The values of μ_0 were calculated for all PMTs together and then for the three PMT types separately (Tab. 1.1). As shown in the table, the different PMT types have distinctly different values of μ_0.

Branch	Average μ_0	μ_0 by PMT type		
		Hamamatsu	HighQENNVT	NNVT
Charge	0.10617±0.00001	0.08621±0.00001	0.11495±0.00001	0.11094±0.00001
nPE_perPMT	0.11819±0.00001	0.10015±0.00002	0.12627±0.00001	0.12194±0.00003
N PMT	0.10337±0.00001	0.09226±0.00001	0.10862±0.00001	0.10481±0.00002

Table 1.1 — The average charge μ_0 per event (1 MeV electron in the center of the detector) per PMT for different branches of the analysis and different PMT types

1.1.3 PMT SENSITIVITIES

Using the acquired values of μ_0 we can extract the sensitivities s_i of each PMT. Using the same generated data sample, we calculate the average charge μ_i collected by the i-th PMT per event and divide it by the respective μ_0 [5]:

$$s_i = \frac{\mu_i}{\mu_0} \tag{1.5}$$

The value of μ_i can be calculated either by taking the ratio of the charge Q_i collected by the i-th PMT to the number of events N_{ev} or by taking the mean value of the Poisson distribution of the p.e. counts in each event, in which case the number of triggers is $N_{trig} = N_{ev}$, because the calculation is performed for each PMT separately.

1.1.4 GEOMETRY OF THE PMT LIGHT COLLECTION MAP

The position of each event can be described using the coordinates $\mathbf{r} = \{x, y, z\}$ (in the detector frame of reference) or the coordinates in the frame of reference of the i-th PMT: the distance L_i between the PMT and event and the polar angle θ_i' at which the PMT «sees» the event (fig. 1.2). We assume axial symmetry of the photocathode sensitivity, thus we do not need a third coordinate (the azimuthal angle) for the PMT frame of reference. Another pair of coordinates can be introduced to describe the event position: the distance from the center of the detector $r = \sqrt{x^2 + y^2 + z^2}$ (which is the same for all the PMTs) and the angle θ_i between $\mathbf{r}$ and $\mathbf{R}_i$ (the position of the i-th PMT in the detector frame of reference).

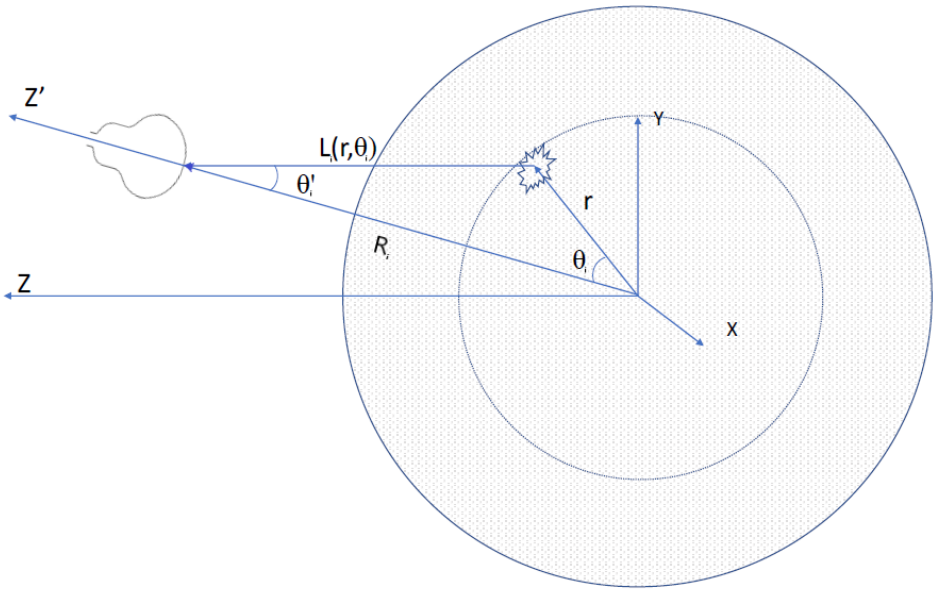

Fig. 1.2 — Positions of a PMT, of an event, and the coordinates used to describe them: $\{r, \cos\theta_i\}$ and $\{L_i, \cos\theta'_i\}$. The shaded volume shows the CD filled with scintillator: a sphere with the radius of $R = 17.7$ m [5]

1.1.5 PMT LIGHT COLLECTION MAP

In [5] the light collection map of each PMT $f_{PMT}(r, \cos\theta_i)$ is defined as the factor, which relates the average charge $\mu_i(r, \cos\theta_i)$ collected by the i-th PMT for an event with coordinates $\{r, \cos\theta_i\}$ to the average charge μ_0 collected by the PMT for an event at the center of the detector:

$$\mu_i(r, \cos\theta_i) = \mu_i \cdot f_{PMT}(r, \cos\theta_i) = \mu_0 \cdot s_i \cdot f_{PMT}(r, \cos\theta_i) \tag{1.6}$$

To determine the light collection map, we generated 400000 events of 1 MeV single electron evenly distributed in the volume of the detector. To approximate the PMT light collection map an analytical function was chosen, following [5]:

$$f_{PMT}(r, \cos\theta) = f_0 \cdot \left(\frac{L(r, \cos\theta)}{L_0}\right)^m \cdot \cos^n\theta'(r, \cos\theta) \cdot \exp\left(-\frac{L(r, \cos\theta) - L_0}{L_{att}}\right) + D \tag{1.7}$$

Here, r and $\cos\theta$ are the coordinates of an event relative to the PMT (Fig. 1.2), f_0 is the normalizing parameter (in order of ≈ 1), $L(r, \cos\theta)$ and $\cos\theta'(r, \cos\theta)$ are the coordinates of the event in the PMT frame of reference, m is a parameter that is either fixed at $m = 2$ (accounts for the solid angle, the light propagation is considered to be isotropic) or is close to 2 (for a slightly better fit), n is a parameter of the fitting function that describes the angular dependency, L_{att} is the parameter representing the attenuation length in the liquid scintillator (in order of ≈ 20 m [8]) and $D \approx 0,09$ is the constant that accounts for the

dark noise of the PMTs (for 30000 s^{-1} dark counts per PMT and 300 ns window of charge collection for each event).

Unfortunately, due to the total internal reflection effect at the edges of the volume of the detector, the fitting procedure only yielded good results in the central part of the detector — up to 10 m from the detector center.

Fit parameter	LPMT type		
	Hamamatsu	HighQENNVT	NNVT
f_0	0.90	0.92	0.92
$m \neq 2$	1.62	2.02	2.02
n	0.68	0.64	0.62
L_{att}	21.6	137.9	131.2
D	0.10	0.08	0.08

Table 1.2 — Parameter values of the analytical approximation 1.7 fit to the generated events histograms

As can be seen from the table, all parameter values, except L_{att}, are close to the expected. To better determine the values of L_{att} an additional analysis of the PMT light collection map was conducted, yielding the same results. As the values $L_{att} \approx 130$ m seem to be incorrect, in the fast generation of events we will be using the value $L_{att} = 21.6$ m.

1.2 FAST GENERATION OF EVENTS

The process of fast generation of events is quite simple. It uses most of the afore mentioned parameters to determine which LPMTs will detect the scintillation event and the charge that will be collected. The JUNO LPMT single photoelectron (SPE) spectre and its parameters are also of great importance:

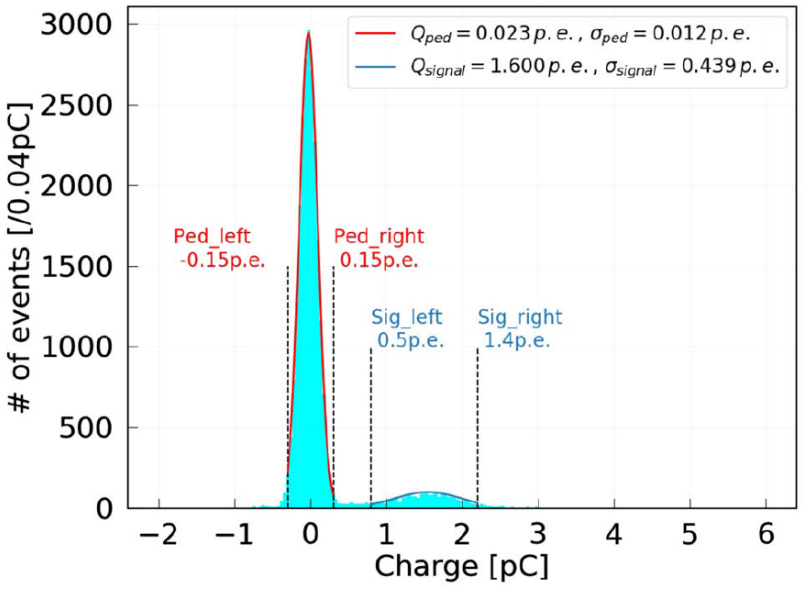

Fig. 1.3 — A typical SPE spectre (charge distribution) of the JUNO LPMTs for $\mu \approx 0.1$ [7]

One of the disadvantages of the fast generation method is that it doesn't generate the times of signals from PMTs. Therefore, there could be no event trigger window established and the signals outside trigger window couldn't be discarded. A simple solution was implemented: from («slowly») generated events the fraction of PMT signals that were inside the trigger window was calculated: 86.72 %; this was implemented in the code for the fast event generation.

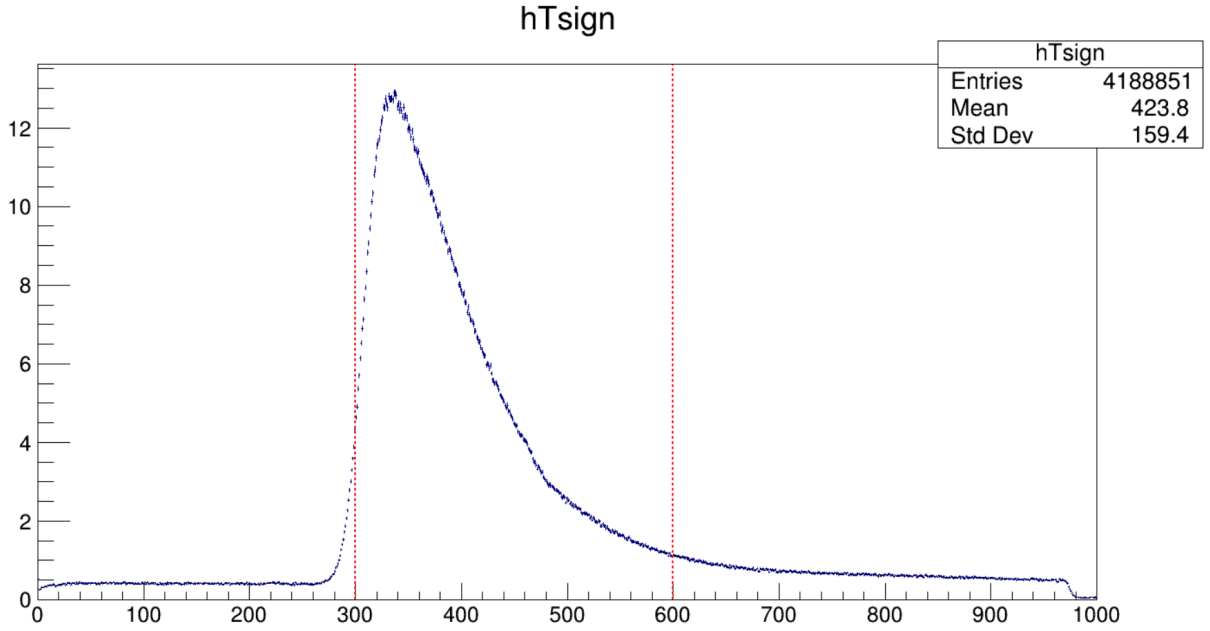

Fig. 1.4 — An average form of the signal from 2000 events of 1 MeV single electron distributed evenly in the volume of the detector (blue) and the trigger window start and end times (red dashed lines).

The algorithm of fast generation:

- random generation of the event coordinates $\mathbf{r} = \{x, y, z\}$ evenly in the chosen ($|\mathbf{r}|< 10$ m, due to best fit) spherically symmetrical volume of the detector;
- a loop for all LPMTs of the CD of JUNO:
  - check if the PMT signal is inside the trigger window; if the i-th PMT signal is outside the trigger window, then the loop continues to the next iteration (i+1-th PMT);
  - depending on i-th PMT type, a random value of μ_0 is generated, using the average value and its error from the table 1.1;
  - the event coordinates $\{L,\cos\theta'\}$ in the frame of i-th PMT are calculated and the average collected charge μ_i is determined using the PMT light collection map (see eq. 1.7) with the parameters corresponding to the i-th PMT type;
  - the number N_{PE} of p.e. collected by the i-th PMT is generated using a Poisson distribution with an average value of μ_i;
  - a loop for N_{PE}:
    - using the single photo electron spectre parameters (see fig. 1.3) and the ENF values [7] of the given PMT type, the collected charge is generated for each

of the collected p.e.;

- the charge collected by the i-th PMT is added to the total charge collected Q by the whole detector and the total charge Q_t collected by the i-th PMT type in this event;
- if $N_{PE} > 0$, the amount N of PMTs of all types and the amount N_t of the PMTs of the i-th PMT type that collected non-zero charge in the event are incremented by 1;

- histograms of Q, Q_t, N and N_t are filled with their appropriate values.

After generating the events, the histograms of charge collected per event and number of PMTs that collected non-zero charge are displayed:

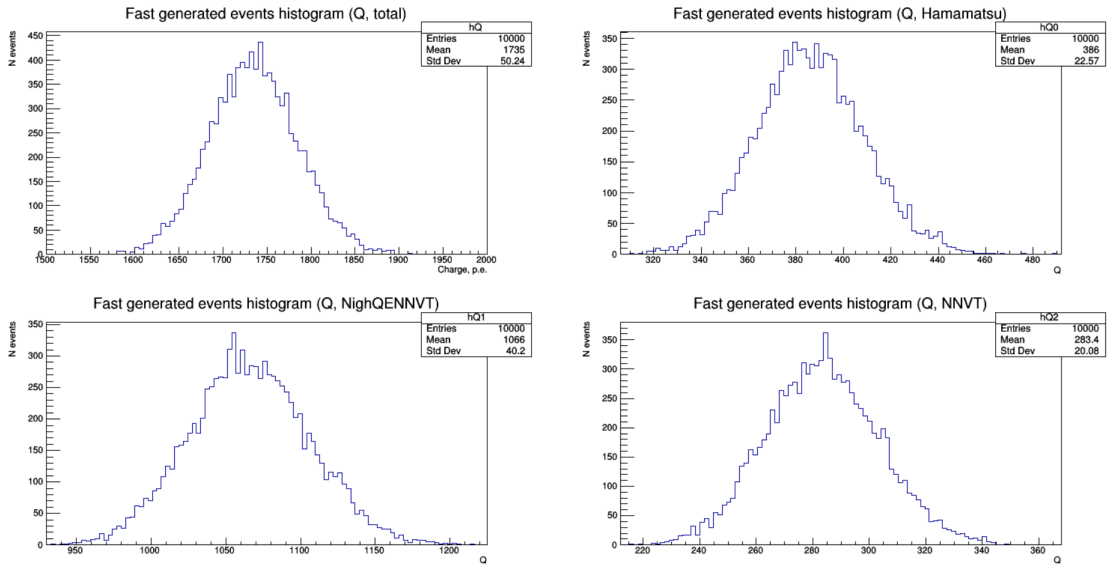

Fig. 1.5 — The distributions of the total collected charge per event for all PMT types (upper left), Hamamatsu (upper right), HighQENNVT (lower left) and NNVT (lower right)

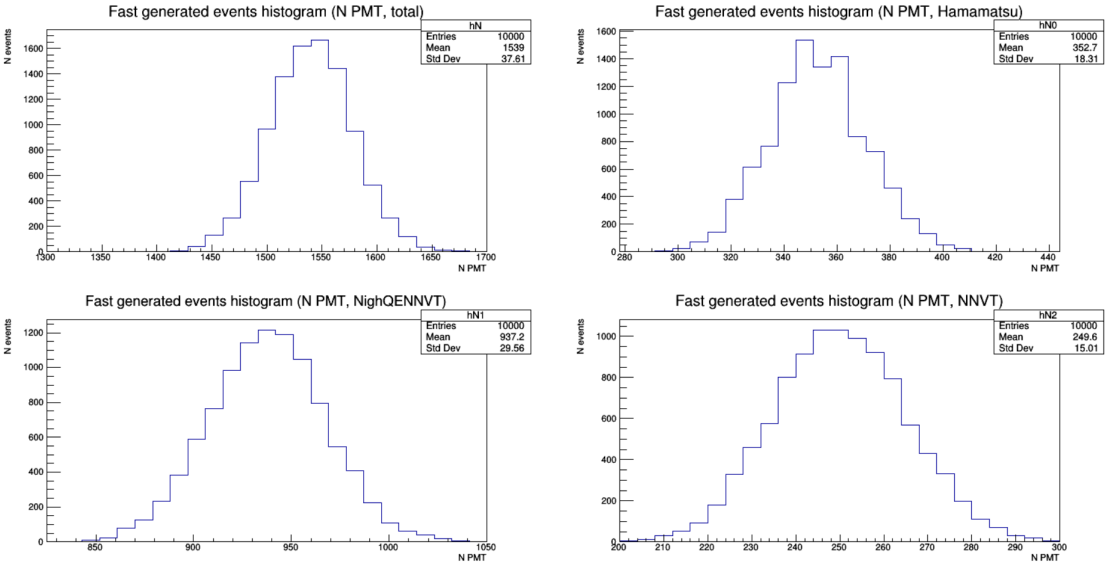

Fig. 1.6 — The distributions of the number of PMTs that collected non-zero charge per event for all PMT types (upper left), Hamamatsu (upper right), HighQENNVT (lower left) and NNVT (lower right)

The estimated amount of p.e. per 1 MeV in an event in JUNO is ≈ 1600. The fast event generator average result of 1735 p.e. contains also the dark noise signals. To estimate their amount we take the event window width of $T = 300$ ns and the dark noise frequency of each PMT of $\nu = 30000$ s^{-1}, then for $N_{PMT} = 17612$ LPMTs of the CD the amount of dark noise signals (or p.e. due to dark noise) in an event is $N_{PMT} \cdot (1 - e^{-T\nu}) \approx 158$. When subtracted from fast generation average result, it gives 1577 p.e. per 1 MeV single electron event, which is in agreement with the expected value.

Comparing the time of fast event generation with the normal event generation gives an excellent result: the time of normal event generation is ≈ 10 s per event, while it takes only 0.05 s to generate 1 event with the fast algorithm, which is 200 times less.

The energy resolution of the detector can be estimated with the results of fast generation. Fitting the histograms of total charge and total amount of PMTs per event (fig. 1.5,1.6, upper left) with a Gaussian function yields dimensionless standard deviations of:

$$\sigma_Q = 2.89\%, \quad \sigma_N = 2.42\%, \tag{1.8}$$

which are again in agreement with the expected JUNO detector energy resolution of $3.02\%/\sqrt{E[MeV]}$.

2 SPATIAL RESOLUTION

2.1 ANALYTICAL APPROXIMATION OF THE SIGNAL FORM

One of the methods of event coordinates reconstruction that was considered in this study, included fitting of the event pulse shape with an analytical approximation. To calculate the needed function, we need to perform a convolution of two functions: first — the normalized distribution of photon emission time in a scintillation:

$$f_1(t) = \left(\frac{A}{\tau_1} e^{\frac{t-T}{\tau_1}} + \frac{1-A}{\tau_2} e^{\frac{t-T}{\tau_2}} \right) \theta(t-T), \tag{2.1}$$

where τ_1, τ_2 are the decay times of the fast and slow components ($\approx$ 10 and 150 ns), A is the fraction of the fast component in the scintillation, T is the time, when the scintillation begins.

The second function is the PMT response:

$$f_2(t, t') = \frac{1}{\sqrt{2\pi}\sigma} e^{-\frac{(t-t')^2}{2\sigma^2}}, \tag{2.2}$$

where σ is the transit time spread parameter of the PMT ($\approx$ 3 and 8 ns for Hamamatsu and NNVT LPMTs, average of 6.8 ns), $t^{'}$ is the true signal time, t is the time when PMT registers a signal.

The convolution of these functions yields:

$$F(t) = \int f_1(t') f_2(t, t') dt' = \frac{A}{2\tau_1} e^{\frac{\sigma^2}{2\tau_1^2}} e^{-\frac{t}{\tau_1}} \left(1 - \operatorname{erf}\left(\frac{T + \frac{\sigma^2}{\tau_1} - t}{\sqrt{2}\sigma} \right) \right) + \\ + \frac{1-A}{2\tau_2} e^{\frac{\sigma^2}{2\tau_2^2}} e^{-\frac{t}{\tau_2}} \left(1 - \operatorname{erf}\left(\frac{T + \frac{\sigma^2}{\tau_2} - t}{\sqrt{2}\sigma} \right) \right) \tag{2.3}$$

However, the above formula doesn't take into account the time of flight (TOF) of the individual photons from the scintillation point to the PMT surface. It turns out that it is much easier to subtract the TOF from the signal time of each individual PMT. To calculate the TOF we need some starting coordinates: an acceptable option is the barycenter of the collected charge in event:

$$\mathbf{B} = \sum_{i=1}^{N_{PMT}} Q_i \mathbf{r}_i \cdot \sqrt{3}, \tag{2.4}$$

where Q_i is the charge collected by the i-th PMT and $\mathbf{r}_i$ are the coordinates of i-th PMT.

2.2 EVENT COORDINATES RECONSTRUCTION

2.2.1 METHOD 1

Both methods of coordinate reconstruction considered in this study involves maximizing the derivative of the event pulse at its front. Firstly, for each event the barycenter is calculated (see eq. 2.4) then the TOF for each signal is derived and a histogram of the (signal time - TOF) with the minimal bin width possible — 1 ns — is filled:

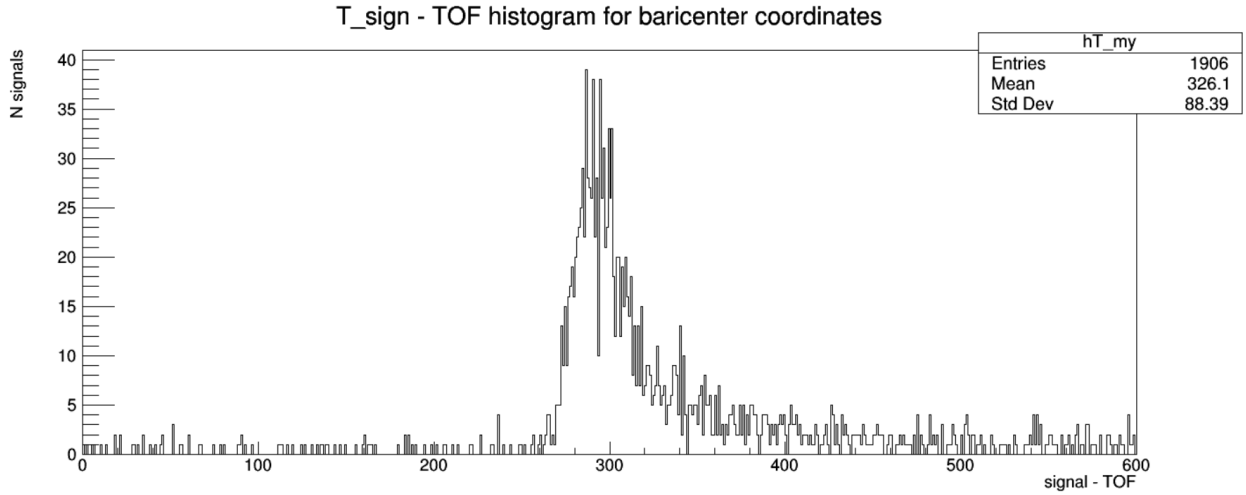

Fig. 2.1 — Histogram of (time of signal arrival - TOF) for 1 MeV single electron event

Following this, the bin with maximum amount of signals is found and the time corresponding to it — t_{max} — as well as the bin, which marks the beginning of the event (the first bin with 7 or more events, as the probability of 7 dark noise events happening in a span of 1 ns is $\approx 1.3 \cdot 10^{-6}$) and the time corresponding to this — t_{start}. Then the approximate center of the front is located at $t_0 = (t_{max} + t_{start})/2$. Taking the derivative of the pulse shape at t_0 we get the value, which should be maximal if the coordinates are close to being true.

To find the best starting point of the maximization process, a few points are randomly generated around the barycenter and the best starting point is chosen among them. Then a simple maximization procedure follows.

For each event the coordinates reconstructed using this method and the true event coordinates are subtracted to find the error of this method. The calculated error is $\Delta r_1 = 1126$ mm. The JUNO implemented method of coordinate reconstruction meanwhile yields an error of $\Delta r_{JUNO} = 159$ mm.

As part of the study of this method, the parameters of the analytical approximation 2.3 were extracted. To do this, the histograms of a small sample of events were added together so that their t_0 points were at 300 ns on the x-axis. This sum was then fitted with 2.3. The results are presented in the following table.

Fit parameter	Parameter value
σ	6.56 ± 0.01
τ_1	8.48 ± 0.05
τ_2	72.1 ± 0.2

Table 2.1 — Parameter values of the analytical approximation 2.3 fit to the sum of generated events pulse shapes

2.2.2 METHOD 2

The other method is very similar to the first one. The difference is that in this method we decided to maximize the maximum of the differences between neighbouring bins of the same histogram. This method was found to work best, if the bin width is larger than in the first method and is equal to 3 ns. The associated error of the method is $\Delta r_2 = 935$ mm, which is slightly better than the first method, but in comparison with the JUNO-implemented method is not great.

This method was also used to find the best value of the refraction index n, which minimizes the error of the method: $n = 1.55$. This value coincides with the refraction index of the scintillator liquid reported by JUNO collaboration [9].

3 CONCLUSION

In the present study

1) a fast event generation algorithm was implemented, which is capable of quickly generating large amounts of events;
2) using the fast event generator, the energy resolution of the JUNO detector was estimated and is in accordance with the expected JUNO energy resolution;
3) 2 similar methods of event coordinates reconstruction were developed and parameters of the PMTs and the scintillator were extracted.

Both methods of event coordinates reconstruction yield significantly worse results than the JUNO-implemented method. This might be due to the internal parameters of the method being non-optimal, hence further study is required.

ACKNOWLEDGMENTS

I thank JINR and the organizing committee of the INTEREST programme for providing an opportunity to work at JINR online, which was a new experience for me.

I am grateful to my supervisor Oleg Smirnov for his guidance and support during the course of this programme.

BIBLIOGRAPHY

1. *JUNO collaboration.* JUNO physics and detector // Progress in Particle and Nuclear Physics. — 2022. — Vol. 123. — P. 103927. — ISSN 0146-6410.
2. Determination of the neutrino mass hierarchy at an intermediate baseline / L. Zhan [et al.] // Phys. Rev. D. — 2008. — Vol. 78, issue 11. — P. 111103.
3. Nuclear physics for geo-neutrino studies / G. Fiorentini [et al.] // Phys. Rev. C. — 2010. — Vol. 81, issue 3. — P. 034602.
4. New experimental limits on violations of the Pauli exclusion principle obtained with the Borexino Counting Test Facility / H. O. Back [et al.] // The European Physical Journal C - Particles and Fields. — 2004. — Vol. 37, no. 4. — P. 421–431. — ISSN 1434-6052.
5. *Смирнов О.* Habilitation thesis - Прямое измерение потока солнечных pp-нейтрино на детекторе Борексино. — URL: https://dissertations.jinr.ru/ru/Dissertations/Announcement/235.
6. *Smirnov O., Kiselev K.* Study of light collection function in JUNO detector. — URL: https://students.jinr.ru/uploads/report_files/report_student_2006_project_364.pdf.
7. Mass testing and characterization of 20-inch PMTs for JUNO / A. Abusleme [et al.] // The European Physical Journal C. — 2022. — Vol. 82, no. 12. — P. 1168. — ISSN 1434-6052.
8. Light attenuation length of high quality linear alkyl benzene as liquid scintillator solvent for the JUNO experiment / H. Yang [et al.] // Journal of Instrumentation. — 2017. — Vol. 12, no. 11. — T11004.
9. Refractive index in the JUNO liquid scintillator / H. S. Zhang [et al.]. — 2024. — arXiv: 2405.19879 [physics.ins-det].